

## Formation of the $S = -1$ resonance $X(2265)$ in the reaction $pp \rightarrow X + K^+$ at 2.50 and 2.85 GeV

P. Kienle<sup>1,2</sup>, M. Maggiora<sup>3</sup>, K. Suzuki<sup>2,a</sup>, T. Yamazaki<sup>4,5</sup>, M. Alexeev<sup>3,14</sup>, F. Balestra<sup>3</sup>, Y. Bedfer<sup>6</sup>, R. Bertini<sup>3,6</sup>, L.C. Bland<sup>7</sup>, A. Brenschede<sup>8</sup>, F. Brochard<sup>6</sup>, M.P. Bussa<sup>3</sup>, M. Chiosso<sup>3</sup>, Seonho Choi<sup>7</sup>, M.L. Colantoni<sup>3</sup>, R. Dressler<sup>13</sup>, M. Dzmidzic<sup>7</sup>, J.-Cl. Faivre<sup>6</sup>, A. Ferrero<sup>3</sup>, L. Ferrero<sup>3</sup>, J. Foryciarz<sup>10,11</sup>, I. Fröhlich<sup>8</sup>, V. Frolov<sup>9</sup>, R. Garfagnini<sup>3</sup>, A. Grasso<sup>3</sup>, S. Heinz<sup>3,6</sup>, W.W. Jacobs<sup>7</sup>, W. Kühn<sup>8</sup>, A. Maggiora<sup>3</sup>, D. Panziera<sup>12</sup>, H.-W. Pfaff<sup>8</sup>, G. Pontecorvo<sup>3,9</sup>, A. Popov<sup>9</sup>, J. Ritman<sup>8</sup>, P. Salabura<sup>10</sup>, V. Tchalyshchev<sup>9</sup>, F. Tosello<sup>3</sup>, S.E. Vigdor<sup>7</sup>, and G. Zosi<sup>3</sup>

<sup>1</sup> Excellence Cluster Universe, Technische Universität München, Garching, Germany

<sup>2</sup> Stefan Meyer Institute for Subatomic Physics, Austrian Academy of Sciences, Vienna, Austria

<sup>3</sup> Dipartimento di Fisica Generale "A. Avogadro" and INFN, Torino, Italy

<sup>4</sup> Department of Physics, University of Tokyo, Tokyo, 113-0033 Japan

<sup>5</sup> RIKEN Nishina Center, Wako, Saitama, 351-0198 Japan

<sup>6</sup> Laboratoire National Saturne, CEA Saclay, France

<sup>7</sup> Indiana University Cyclotron Facility, Bloomington, Indiana, USA

<sup>8</sup> II. Physikalisches Institut, Universität Gießen, Germany

<sup>9</sup> JINR, Dubna, Russia

<sup>10</sup> M. Smoluchowski Institute of Physics, Jagellonian University, Kraków, Poland

<sup>11</sup> H. Niewodniczanski Institute of Nuclear Physics, Kraków, Poland

<sup>12</sup> Università del Piemonte Orientale and INFN, Torino, Italy

<sup>13</sup> Forschungszentrum Rossendorf, Germany

<sup>14</sup> INFN, Trieste, Italy

Received: 7 June 2012 / Revised: 21 October 2012

Published online: 12 December 2012

© The Author(s) 2012. This article is published with open access at Springerlink.com

Communicated by T. Hennino

**Abstract.** Analyzing DISTO data of  $pp \rightarrow p\Lambda K^+$  at  $T_p = 2.50$  and  $2.85$  GeV to populate a previously reported  $X(2265)$ -resonance with  $M_X = 2267$  MeV/ $c^2$  and  $\Gamma_X = 118$  MeV at  $2.85$  GeV, we found that the yield of  $X(2265)$  at  $2.50$  GeV is much less than that at  $2.85$  GeV (less than 10%), though it is expected from a kinematical consideration to be produced as much as 33% of that at  $2.85$  GeV. The small population of  $X(2265)$  at  $2.50$  GeV is consistent with the very weak production of  $\Lambda(1405)$  at the same incident energy toward its production threshold, thus indicating that  $\Lambda(1405)$  plays an important role as a doorway state for the formation of  $X(2265)$ .

Recently, analyzing a set of the DISTO data of an exclusive reaction,  $pp \rightarrow p\Lambda K^+$ , taken at an incident kinetic energy of  $T_p = 2.85$  GeV, we found [1] a broad resonance with a mass of  $M_X = 2267 \pm 2(\text{stat}) \pm 5(\text{syst})$  MeV/ $c^2$  and a width of  $\Gamma_X = 118 \pm 8(\text{stat}) \pm 10(\text{syst})$  MeV, in the invariant-mass spectrum  $M(p\Lambda)$ , and also in the missing-mass spectrum  $\Delta M(K^+)$ . For the time being, we call this resonance  $X(2265)$ . An indication for a similar resonance in  $K^-$  absorption by light nuclei was reported by FINUDA [2].

For further understanding the nature of  $X(2265)$  we studied the entrance-channel behavior of the  $pp$  reaction, and analyzed more experimental data from DISTO taken

at  $2.50$  GeV. At this energy the formation of  $X(2265)$  should still be kinematically allowed (the nominal threshold energy:  $T_p^{\text{thres}}(X(2265)) = 2.19$  GeV), whereas the formation of the  $\Lambda(1405)$ -resonance (abbreviated here as  $\Lambda^*$ ) is expected to become very weak toward its production threshold ( $T_p^{\text{thres}}(\Lambda^*) = 2.42$  GeV). This will clarify the nature of  $X(2265)$  and let us know if the  $\Lambda^*$  plays an essential role in its formation process.

The DISTO experiment was carried out with the SATURNE accelerator at Saclay [3,4]. Here, we have analyzed the data set of the exclusive reaction products  $p\Lambda K^+$  at  $T_p = 2.50$  GeV, and compared the results with those at  $2.85$  GeV [1,5] using the same analysis method and checking the acceptance corrections at both incident energies. About 125k exclusive events were selected from

<sup>a</sup> e-mail: ken.suzuki@oeaw.ac.at

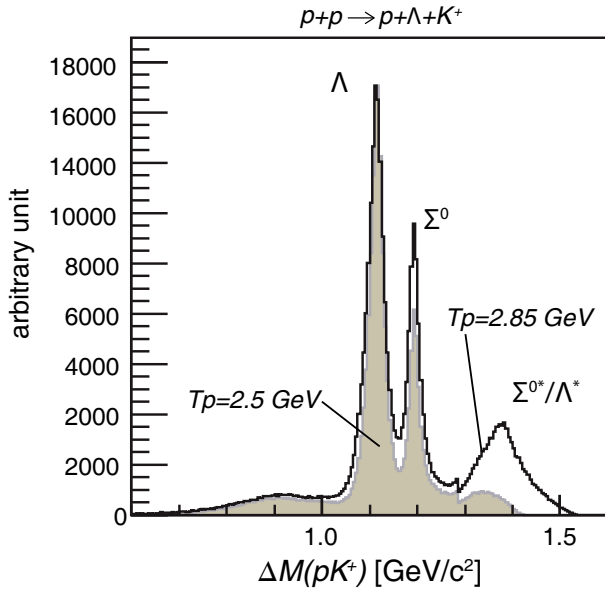


**Fig. 1.** Comparison of missing-mass  $\Delta M(pK^+)$  spectra of the  $pp \rightarrow p\Lambda K^+$  reaction at  $T_p = 2.85 \text{ GeV}$  (solid histogram) and  $2.50 \text{ GeV}$  (shaded) normalized to the numbers of observed  $\Lambda$ 's.

a neutral hyperon missing-mass spectrum  $\Delta M(pK^+)$ , using the previous procedures described in detail in [1, 5].

Figure 1 shows missing-mass spectra  $\Delta M(pK^+)$  at  $T_p = 2.85$  and  $2.50 \text{ GeV}$ . The momentum distributions of the two particles,  $p$  and  $\Lambda$ , are examined to prove that the momentum acceptance for  $\Delta M(pK^+)$  is flat at both incident energies. Thus, the cut-off of the missing-mass spectrum  $\Delta M(pK^+)$  at  $1.4 \text{ GeV}/c^2$  for  $T_p = 2.50 \text{ GeV}$  is found not to be due to a change of the momentum acceptance of the  $p$  and  $K^+$ . The  $\Delta M(pK^+)$  spectrum at  $2.85 \text{ GeV}$  shows peaks at masses of  $\Lambda$ ,  $\Sigma^0$ , and  $\Sigma^0(1385) (\equiv \Sigma^{0^*}) + \Lambda(1405) (\equiv \Lambda^*)$ , the latter two being unresolved.

Zychor *et al.* [6] made an analysis on their  $\Sigma^{0^*} + \Lambda^*$  composite peak in  $pp \rightarrow p\Lambda K^+$  events at  $2.83 \text{ GeV}$ , and found that it is composed of  $\Sigma^{0^*}$  and  $\Lambda^*$  by an intensity ratio of  $I(\Lambda^*) : I(\Sigma^{0^*}) = 1.00 : 2.37$ . They used the missing-mass information for  $\pi^0$  and  $\Sigma^0 \rightarrow \Lambda\gamma$  to distinguish between  $\Sigma^{0^*} \rightarrow \Lambda\pi^0$  and  $\Lambda^* \rightarrow \Sigma^0\pi^0 \rightarrow \Lambda\gamma\pi^0$ , and obtained the individual cross-sections as  $\sigma(\Sigma^{0^*}) = 4.0 \mu\text{b}$  and  $\sigma(\Lambda^*) = 4.5 \mu\text{b}$ .

The  $\Delta M(pK^+)$  spectrum at  $2.50 \text{ GeV}$ , which is overlaid in fig. 1, shows again the signals for the production of  $\Lambda$  and  $\Sigma^0$ , but the  $\Sigma^{0^*} + \Lambda^*$  complex bump appears to be very much reduced and shifted toward lower mass; obviously, the formation of the  $\Lambda^*$  resonance is kinematically hindered toward the threshold ( $T_p^{\text{thres}}(\Lambda^*) \sim 2.42 \text{ GeV}$ ) at an incident energy of  $2.50 \text{ GeV}$ . The dramatic change of the  $\Lambda^*$ -resonance shape and intensity at  $T_p = 2.50 \text{ GeV}$  is understood by considering the finite width of  $\Lambda^*$ . By assigning the whole shaded area above  $\Delta M(pK^+) = 1.3 \text{ GeV}/c^2$  to  $\Lambda^* + \Sigma^{0^*}$  production, we assume an upper limit on the ratio of  $\Lambda^*$  production at  $T_p = 2.50$  and  $2.85 \text{ GeV}$  of 0.10.

For the analyses of the reaction spectra, we take an acceptance-uncorrected raw experimental spectral distribution ( $RAW^{(\alpha)}$ ) for a given two- or one-dimensional variable,  $\alpha$ , such as the Dalitz variables or their projections, and a corresponding simulated distribution ( $SIM^{(\alpha)}$ ) calculated for events of the three-body reaction  $p\Lambda K^+$  assuming a uniform phase-space distribution, folded with the DISTO geometrical acceptance. To avoid possible uncertainties in the acceptance correction, we adopt a *deviation spectrum* method to obtain an acceptance-compensated presentation of the spectrum of  $\alpha$ , by calculating

$$DEV^{(\alpha)} = RAW^{(\alpha)} / SIM^{(\alpha)} \quad (1)$$

for all bins. A thus obtained  $DEV$  spectrum is not only acceptance compensated, but also is free from dropping phase-space densities (bell shaped) near their boundaries. A  $DEV$  spectrum is in general flat and linear, but will reveal a non-linear structure when a physically meaningful deviation from a uniform phase-space distribution occurs, such as a resonance.

From the previous analysis we learned that all  $p\Lambda K^+$  events are clearly distinguished by their proton angular distribution, which consists of a sharp forward/backward peaked component and a flat large-angle component [1]. The observed angular distribution of protons is explained by considering the ordinary reaction process,

$$p + p \rightarrow p + \Lambda + K^+, \quad (2)$$

without invoking resonances. A simple estimation of the angular distribution and the  $M(p\Lambda)$  spectrum is used here [7], and explained in what follows. All the kinematical variables are given in the c.m. frame. The incident proton with a momentum of  $\hbar\mathbf{k}_0$  produces a scattered proton with energy momentum  $E_1, \hbar\mathbf{k}_1$ , a  $\Lambda$  particle with  $E_2, \hbar\mathbf{k}_2$  and a  $K^+$  with  $E_3, \hbar\mathbf{k}_3$ . The momentum transfer from the incident proton to the scattered proton,  $Q = |\mathbf{k}_0 - \mathbf{k}_1|$  is given by

$$Q^2 = k_0^2 + k_1^2 - 2k_0k_1X_1, \quad (3)$$

with  $X_1 = (\hat{k}_0 \cdot \hat{k}_1)$ . The cross-section of the process  $pp \rightarrow p\Lambda K^+$  is given by a  $T$ -matrix, which depends on  $Q^2$ , as

$$T(Q^2) = V_0 \left[ \frac{1}{1 + b_1^2 Q^2} + G \frac{1}{1 + b_2^2 Q^2} \right], \quad (4)$$

where

$$b_1 = \frac{\hbar c}{m_B^{(1)}}, \quad b_2 = \frac{\hbar c}{m_B^{(2)}}, \quad (5)$$

with  $V_0$  representing the interaction strength, and  $m_B^{(1)}$  and  $m_B^{(2)}$  being representative intermediate boson masses effective for small and large momentum transfers, respectively. The observed very sharp forward and backward peaked components of the proton angular distribution [1] are well accounted for by postulating  $m_B^{(1)} \approx m_\pi$  and  $G = 0$ .

Since the proton angular distribution in the ordinary background process is forward peaked, we made a strategy to divide observed events according to "Large Angle

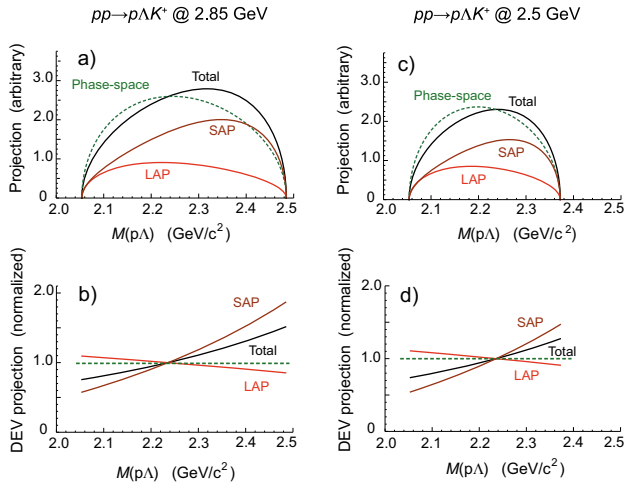


**Fig. 2.** (Colour on-line) (Top: a, c) Simulated distributions of  $M(p\Lambda)$  (without acceptance correction) for various proton angle groups (LAP, SAP and Total) at  $T_p = 2.85$  GeV (a, b) and 2.50 GeV (c, d), calculated for the ordinary three-body process with an intermediate boson mass of  $m_B^{(1)} = m_\pi$  and  $G = 0$ . (Bottom: b, d) Corresponding calculated  $DEV$  presentations of  $M(p\Lambda)$  spectra. The case of homogeneous distributions over phase space is shown by dashed curves in a) and c), and by dashed horizontal lines in b) and d).

Proton” and “Small Angle Proton” cuts, denoted by LAP with  $|\cos\theta_{\text{cm}}(p)| < 0.6$ , and by SAP with  $|\cos\theta_{\text{cm}}(p)| > 0.6$ , respectively. In fact, we have found that the observed Dalitz plots (not shown here) depend very much on the selection of the proton angular ranges [1].

The dependence of the cross-section on the Dalitz variables,  $x_{p\Lambda} \equiv M^2(p\Lambda)$  and  $y_{K\Lambda} \equiv M^2(K\Lambda)$ , which are uniquely related to the momenta of  $K^+$  and  $p$ , through  $\mathbf{k}_3$  and  $\mathbf{k}_1$ , respectively, is expressed in terms of  $T(Q^2)$ ,

$$\frac{d^2\sigma}{dx_{p\Lambda} dy_{K\Lambda}} = \text{const} \int |T(Q^2)|^2 dX_1. \quad (6)$$

This formula expresses in the simplest way that the Dalitz density depends on  $|T(Q^2)|^2$  and becomes flat when  $m_B$  is large. The distributions for selected proton angular ranges can be reproduced by integrating over  $X_1$ . The  $M(p\Lambda)$  distribution of the Dalitz plot can be evaluated by integration of eq. (6) over  $y_{K\Lambda}$ .

The calculated distributions (without acceptance corrections) and their  $DEV$  presentations at  $T_p = 2.85$  and 2.50 GeV are shown in fig. 2 for Total, LAP and SAP groups, as well as for the uniform phase-space. All the projection distributions of  $M(p\Lambda)$  (upper panels: a, c) are bell shaped, and thus, not easily distinguishable. On the other hand, their  $DEV$  presentations (lower panels: b, d) are nearly linear with easily distinguishable different gradients, which are shown to correspond to different proton angular distributions, reflecting different momentum transfers. Furthermore, for actual experimental data ( $RAW$ ) the  $DEV$  distributions are acceptance compensated, as  $SIM$  data take into account the acceptance realistically. The distributions for 2.85 GeV and 2.50 GeV

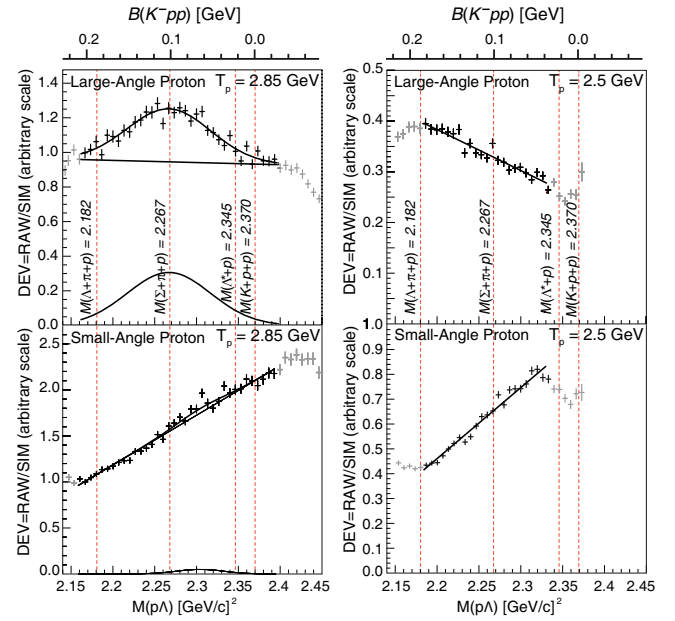
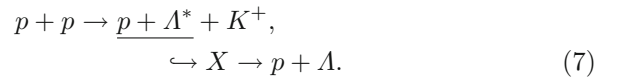


**Fig. 3.** Invariant-mass spectra ( $DEV = RAW/SIM$  of  $M(p\Lambda)$ ) in arbitrary units for  $T_p = 2.85$  GeV (left) and 2.50 GeV (right) incident energies. The upper and lower spectra were obtained by applying Large Angle Proton (LAP) and Small Angle Proton (SAP) selections, respectively. The thresholds of some relevant decay channels are shown by vertical dashed lines. The points in light grey outside the solid fit zones were discarded because, there, the  $DEV$  ratios are not reliable due to the rapidly decreasing acceptance at its boundaries, causing larger systematic errors that cannot be easily assessed.

incident energies (shown in left panels, a, b and right panels, c, d of fig. 2, respectively) are similar to each other.

The flat large-angle component (LAP) can also be explained as the ordinary process (2) with large  $m_B$  values, but it may in addition involve an exotic two-body process via a  $p\Lambda^*$  doorway state to a resonance  $X$ ,



The existence of such an  $X$  can be signaled as a peak in both invariant-mass  $M(p\Lambda)$  and missing-mass  $\Delta M(K^+)$   $DEV$  spectra.

Figure 3 shows a comparison of the invariant-mass  $DEV$  spectra of  $M(p\Lambda)$  for  $pp$  collisions at incident energies of  $T_p = 2.85$  GeV (left panels) and 2.50 GeV (right panels). The upper spectra at both energies are with LAP selections, involving a much smaller contribution of the ordinary background, eq. (2). This selection should not cause any fake effect on the mass spectra, because the proton momentum in c.m. is not so different between the two incident energies; the purpose of the selection is to remove a large amount of extreme forward and backward protons, which are the main source of the background. In fact, the SAP spectra of both incident energies (the lower spectra of fig. 3) show linear behaviors of similar positive gradients without a resonant peak. This tendency is the characteristic feature of the ordinary reaction, eq. (2),

when mediated by a low-mass intermediate boson. Figure 2 shows the calculated  $M(p\Lambda)$  distributions (upper panels) and their *DEV* presentations (lower panels) at  $T_p = 2.85$  and  $2.50$  GeV for  $m_B^{(1)} \approx m_\pi$  and  $G = 0$  (no large  $m_B^{(2)}$ ) for different proton-angle groups (LAP, SAP and Total) as well as for uniform phase-space.

We find a striking difference in the *DEV* invariant-mass spectra,  $M(p\Lambda)$ , of LAP between  $T_p = 2.85$  and  $2.50$  GeV. The  $M(p\Lambda)$  spectrum at  $2.85$  GeV shows an outstanding peak that we identified in [1] as the production of a resonance,  $X(2265)$ , with high transverse momentum protons in the two-body  $p+p \rightarrow X+K^+$  reaction followed by  $X \rightarrow p+\Lambda$ , eq. (7). In contrast to this behavior, at  $2.50$  GeV nearly no trace of the  $X(2265)$  contribution is visible. The  $M(p\Lambda)$  spectra of both SAP and LAP are totally flat in the mass region of the  $X(2265)$  peak; the latter (LAP) shows a negative slope, which is consistent with the simulation given in fig. 2 (c, d), and may also reflect a final-state interaction effect between  $p$  and  $\Lambda$  [8]. To extract the yield, a fit was made with a Gaussian peak, representing the  $X(2265)$  process (7) plus a linear background for the three-body process (2), on the  $M(p\Lambda)$  spectra at both incident energies. The  $\Delta M(K^+)$  missing-mass spectra show the same behavior as the  $M(p\Lambda)$  invariant-mass spectra presented here.

The yield of the peak  $X$  versus the  $p\Lambda K^+$  background, defined as

$$Y_X(T_p) = \frac{\text{Peak intensity in } DEV}{\text{BG intensity in } DEV}, \quad (8)$$

is estimated to be

$$Y_X(2.85) = 0.168 \pm 0.010, \quad Y_X(2.50) = 0.002 \pm 0.021, \quad (9)$$

and thus the  $T_p$  dependence of  $Y$  is expressed by the ratio

$$\frac{Y_X(2.50)}{Y_X(2.85)} = 0.012 \pm 0.125. \quad (10)$$

The peak-to-background ratios,  $Y_X(T_p)$ , are scaled by the cross-section  $\sigma_{p\Lambda K}(T_p)$  for reaction (2), which can be derived from the  $T_p$  dependence of the  $\Lambda$  cross-section, as can be seen in fig. 4. Note that there are even measured cross-sections at energies close by. Then, the ratio of the cross-section for  $X(2265)$  at  $2.50$  and  $2.85$  GeV is obtained as

$$\begin{aligned} R_X^{\text{obs}} &= \frac{\sigma_X(2.50)}{\sigma_X(2.85)} = \frac{Y_X(2.50)}{Y_X(2.85)} \times \frac{\sigma_{p\Lambda K}(2.50)}{\sigma_{p\Lambda K}(2.85)} \\ &= 0.009 \pm 0.091, \end{aligned} \quad (11)$$

where the value for the  $\Lambda$  production cross-section ratio of  $0.73$ , obtained from fig. 4, is used. To be consistent with the error bar, we consider an upper limit including one standard deviation, that is,  $R_X^{\text{obs}} < 0.10$ . Note that, despite a possible difference of the detector acceptance at  $2.85$  and  $2.50$  GeV, the peak yield,  $Y_X(T_p)$ , deduced from a *DEV* spectrum is acceptance compensated.

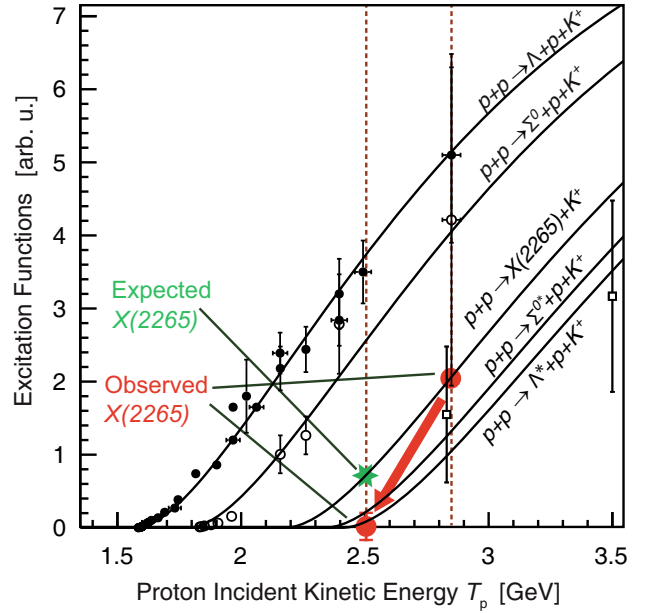


**Fig. 4.** Relative excitation functions in arbitrary units of the reactions  $p+p \rightarrow p+\Lambda+K^+$ ,  $\rightarrow p+\Sigma^0+K^+$ ,  $\rightarrow X(2265)+K^+$ ,  $\rightarrow p+\Sigma^{0*}+K^+$  and  $\rightarrow p+\Lambda^*+K^+$ . The curves are drawn by using a universal formula [9], eq. (12), on which known experimental points with error bars of  $\Lambda$  (full circles) and  $\Sigma^0$  (open circles) [8] are fitted and located. The data for  $\Lambda(1405)$  production [6, 10] are also shown. The upper limit of the  $\Lambda^*$  production ratio of  $T_p = 2.50$  GeV to  $2.85$  GeV,  $0.10$ , derived from fig. 1, is consistent with the  $\Lambda^*$  production curve. The observed relative cross-sections for  $X(2265)$  at  $2.50$  and  $2.85$  GeV are shown by large red circles, and the expected one at  $2.50$  GeV relative to that at  $2.85$  GeV is shown by a green star. The bold red arrow indicates the present observation, which is significantly different from the universal curve for the  $X(2265)$  production.

To further discuss the implication of this experimental result, we consider the excitation functions ( $T_p$  dependence of the relative production cross-sections) of various strange particles of mass  $M$ . Figure 4 shows the excitation functions in arbitrary units for the reactions  $p+p \rightarrow \Lambda+p+K^+$ ,  $\rightarrow \Sigma^0+p+K^+$ ,  $\rightarrow X(2265)+K^+$ ,  $\rightarrow p+\Sigma^{0*}+K^+$  and  $\rightarrow \Lambda^*+p+K^+$ . They are drawn following a semi-empirical universal form of Sibirtsev [9] as a function of the center-of-mass energy ( $\sqrt{s}$ ) common to each with different thresholds ( $\sqrt{s_0} = M + m_p + m_K$ ), as expressed by

$$\sigma(s) = \sigma_0 \times \left(1 - \frac{s_0}{s}\right)^\alpha \times \left(\frac{s_0}{s}\right)^\beta, \quad (12)$$

with two parameters,  $\alpha$  and  $\beta$ , and a constant,  $\sigma_0$ . It is consistent with what is expected from a simple phase-space dependence. The curves shown are for the best-fit parameters,  $\alpha = 1.8$  and  $\beta = 1.5$ , which we have found using empirical data for  $\Lambda$  (full circles) and  $\Sigma^0$  (open circles) productions [8]. From these curves one would expect the following ratio for the cross-sections of  $X(2265)$  at  $2.50$

and 2.85 GeV,

$$R_X^{\text{expected}} = \frac{\sigma_X(2.50)}{\sigma_X(2.85)} \approx 0.33, \quad (13)$$

if  $X$  is an ordinary object that would follow the above relation (12). This is in strong disagreement with the experimental upper limit,  $R_X^{\text{obs}} < 0.10$ .

Another way to consider the  $T_p$  dependence of the  $X(2265)$  cross-section is as follows. Whereas the  $X(2265)$  peak at 2.85 GeV is located close to the left-lower edge of the Dalitz domain (see fig. 1 of ref. [1]), the same position of  $X(2265)$  at 2.5 GeV is rather central of the Dalitz domain that moves toward smaller  $M(p\Lambda)$  and  $M(K^+\Lambda)$  values so that even a larger cross-section ratio may be expected, reflecting the larger phase-spaces of the decay particles,  $(p\Lambda) + (K^+\Lambda)$ . Of course, such an expectation is opposite to the experimental finding.

In summary, we studied the  $T_p$  dependence of  $X(2265)$  production, and found that the formation cross-section at 2.50 GeV is much less than at 2.85 GeV. The origin of this observation may be related to the fact that the formation of a real  $\Lambda^*$ -resonance drops down at 2.50 GeV. This view is consistent with the proposed picture on the role played by  $\Lambda^*$  as an essential constituent of a kaonic nuclear bound state,  $K^-pp$  [11], and as a doorway particle for the production of  $K^-pp$  in  $pp$  reactions [12]. On the other hand, one might wonder if the presence of nucleon resonances which decay partially to  $K^+\Lambda$ , such as  $N^*(1650)$  and  $N^*(1710)$  [8], may cause a fake resonance pattern in  $M(p\Lambda)$ . We actually observe such  $N^*$ -resonances in DISTO data, but we have confirmed from simulations that their reflections do not produce any fake peak in the  $M(p\Lambda)$  distributions. This view is supported by the fact that no peak in  $M(p\Lambda)$  is seen at  $T_p = 2.5$  GeV, although the  $N^*$  resonances are still observed at the lower bombarding energy. These aspects will be reported elsewhere in the near future.

We are indebted to a stimulating theoretical discussion with Professor Y. Akaishi. This research was partly supported by the DFG cluster of excellence ‘‘Origin and Structure of the Universe’’ of Technische Universitat Munchen and by Grant-in-Aid for Scientific Research of Monbu-Kagakusho of Japan. One of us (TY) acknowledges support by an Award of the Alexander von Humboldt Foundation, Germany, and as a visiting Fellow of the Institute for Advanced Study of the Technische Universitat Munchen.

**Open Access** This is an open access article distributed under the terms of the Creative Commons Attribution License (<http://creativecommons.org/licenses/by/3.0>), which permits unrestricted use, distribution, and reproduction in any medium, provided the original work is properly cited.

## References

1. T. Yamazaki *et al.*, Phys. Rev. Lett. **104**, 132502 (2010).
2. M. Agnello *et al.*, Phys. Rev. Lett. **94**, 212303 (2005).
3. F. Balestra *et al.*, Nucl. Instrum. Methods A **426**, 385 (1999).
4. M. Maggiora *et al.*, Nucl. Phys. A **691**, 329c (2001).
5. M. Maggiora *et al.*, Nucl. Phys. A **835**, 43 (2010).
6. I. Zychor *et al.*, Phys. Lett. B **660**, 167 (2008).
7. Y. Akaishi, private communication (2009).
8. S. Abd El-Samad *et al.*, Phys. Lett. B **688**, 142 (2010).
9. A. Sibirtsev, Phys. Lett. B **359**, 29 (1995).
10. G. Agakishiev *et al.*, to be published in Phys. Rev. C, arXiv-1208.0205v1.
11. T. Yamazaki, Y. Akaishi, Phys. Lett. B **535**, 70 (2002).
12. T. Yamazaki, Y. Akaishi, Phys. Rev. C **76**, 045201 (2007).